IJE TRANSACTIONS B: Applications Vol. 37 No. 02, (February 2024) 283-297

International Journal of Engineering

Journal Homepage: www.ije.ir

Optical Efficiency of Linear Fresnel Reflectors in Fixed, Variable and Optimal Distance between Mirrors: Theoretical and Experimental Studies

A. Nakhaei Zadeh[a], M. Ameri*[a], A. Shojaei[a], I. Baniasad Askari[b]

[a] *Department of Mechanical Engineering, Shahid Bahonar University of Kerman, Kerman, Iran*
[b] *Department of Mechanical Engineering, University of Zabol, Iran*

P A P E R I N F O

Paper history:
Received 10 August 2023
Received in revised form 23 September 2023
Accepted 23 September 2023

Keywords:
Linear Fresnel Reflectors
Solar Concentrators
Optical Efficiency
Thermal Efficiency
Optimization

A B S T R A C T

In linear Fresnel reflectors, field arrangement has a significant effect on optical efficiency. Three constant, optimal, and variable distance layouts are proposed for Fresdemo solar power plant. The study was carried out by simulation and experiment. The small-scale Fresnel concentrator was designed and built with the capability to implement these three arrangements. The optical efficiency of the solar power plant with optimal variable and constant gap between mirrors were compared, considering fixed conditions for all layouts, including overall dimensions of the plant, width, and number of mirrors and dimensions of the receiver. It was observed that the arrangement with the optimal variable, and fixed distance had the highest to the lowest energy efficiency. Besides, the mirrors farther from the center entail more losses due to the sharper tilt angles, hence more spaces between these mirrors is required to reduce the losses. Meanwhile, the last mirrors in fixed distance arrangement have severe losses of shading and blocking while, they produce almost the same energy as central mirrors in the optimal and variable distance arrangement. The experimental results of the developed prototype showed that the thermal efficiency for the optimal distance was the highest, while it was followed closely by variable distance arrangement. The fixed distance arrangement had the lowest thermal efficiency. In addition, the variable and optimal distance arrangements exhibited an efficiency of 54% and 55%, respectively.

***doi**: 10.5829/ije.2024.37.02b.06*

Graphical Abstract

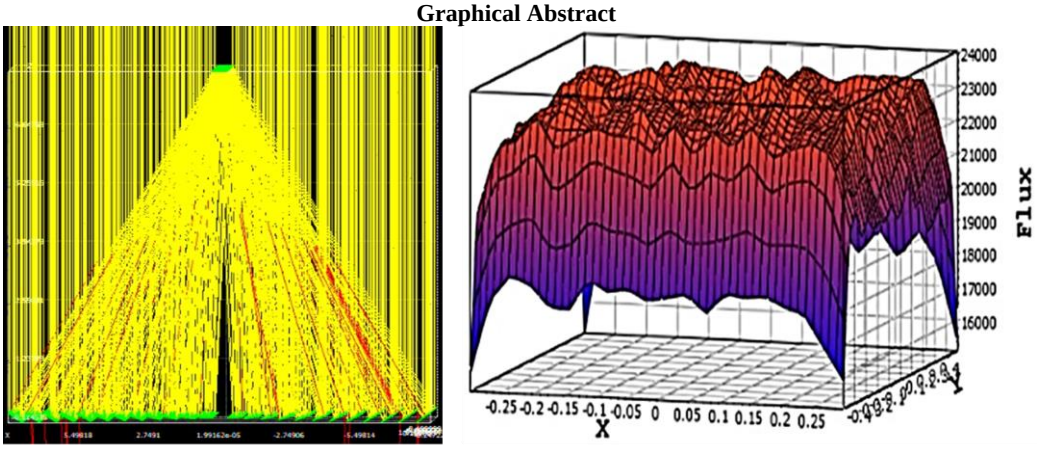

a) Ray-Tracing simulation b) Solar radiation distribution on the LFR receiver

*Corresponding Author Email: *ameri_mm@uk.ac.ir* (M. Ameri)

Please cite this article as: Nakhaei Zadeh A, Ameri M, Shojaei A, Baniasad Askari I. Optical Efficiency of Linear Fresnel Reflectors in Fixed, Variable and Optimal Distance between Mirrors: Theoretical and Experimental Studies, International Journal of Engineering, Transactions B: Applications. 2024;37(02):283-97.

NOMENCLATURE

A_a	Absorber area (m^2)	q	Distance from the center of the field (m)
AFSC	Annular Fresnel solar concentrators	$\hat{S}$	Angle of the Sun's rays above the horizon on the transverse plane
AFSCF	Annular Fresnel solar concentrator coupled with a circular Fresnel lens	SPT	Solar Power Tower
B	Receiver's width (m)	s_n	Distance between two consecutive mirrors (m)
CSP	Concentrated Solar Power	T	Absolute temperature (K)
C_p	Specific heat at constant pressure (J/kg ℃)	T_i	Inlet temperature (K)
DNI	Direct Normal Irradiance, (W/m^2)	PTC	Parabolic Trough Collector
f	The height of absorber (m)	PDC	Parabolic Dishes Collector
f_b	The ratio of the blocked area of a mirror by the adjacent mirror to mirror surface	q	Distance from the center of the field (m)
f_s	The ratio of the shadowed area of a mirror by the adjacent mirror to mirror surface	T_o	Outlet temperature (K)
f_t	Total Loss Factor	T_a	Ambient temperature (K)
GA	Genetic algorithm	VDA	Variable distance arrangement
G_b	Beam radiation (W/m^2)	w_{nb}	The amount of unblocked area of a mirror (m^2)
LFC	Linear Fresnel Collector	w_{ns}	The amount of unshaded area of a mirror (m^2)
LFR	Linear Fresnel Reflector	**Greek Symbols**	
$\dot{m}$	Mass flow rate of fluid (kg/s)	$\widehat{\beta_l}$	Angle between the axis perpendicular to the mirror and horizon
$\widehat{M_l}$	Slope of the mirrors	$\widehat{\gamma_R}$	Angle of the line connecting the mirror center and receiver center with the horizon
ODA	Optimal distance arrangement	$\hat{\theta}$	Angle of the mirrors in the first generation of Fresnel collectors
PTC	Parabolic Trough Collector	η	Collector efficiency
PDC	Parabolic Dishes Collector	$\hat{\xi}$	Angle of inclination of the sun's rays

1. INTRODUCTION

The fast pace of technology and population growth have led to escalating CO_2 pollution, global warming, and fossil fuel depletion (1). Therefore, the use of renewable energy resources seems to be promising for electricity generation or water desalination (2, 3). Two different categories are usually defined for solar power plants, concentrating solar power plants (CSP) and photovoltaic systems (4). CSPs concentrate the solar energy on a fluid using different reflective instruments, leading to the generation of electrical energy based on the heated fluid in the turbine (5). The CPSs are divided into four categories concerning the geometrical characterization of reflectors, including parabolic dish collector (PDC), solar power tower (SPT) (6), parabolic trough collector (PTC), linear Fresnel collector (LFC) (7).

LFCs are a type of linear concentrating system with flat or slightly curved mirrors. The tilt of the mirrors changes to concentrate sunlight on the receiver in the center of the field. Two different generations have been developed for LFCs (8). In the first one, the fixed mirrors are arranged on a moving plate and the plate tracks the sun. In the second type, the mirrors reflect the sunlight on the receivers by changing their tilt. The first type became obsolete due to manufacturing difficulties and subsequent research was conducted on the second type. Losses of Fresnel collectors are divided into two categories: optical losses and thermal losses. The optical losses account for a larger share than thermal losses since these collectors usually are used at low and medium temperatures (9, 10). Fresnel systems are usually compared with linear parabolic collectors. A comparison of the advantages and disadvantages of LFCs and linear parabolic systems is summarized in Table 1.

The ease of construction and reduced costs of maintenance are the most critical advantages of linear Fresnel concentrators. Several parameters including the length and width of the mirrors, their distance from each other, receiver height, field position (north-south or east-west), field gradient, and number of mirrors are defined in the design process. The parameters not only provide designers with more freedom but also increase the complexity of design analysis and optimization. Therefore, these parameters need to be addressed in-depth to reduce losses in collectors and maximize collector efficiency based on Bellos et al. [9]. Every single parameter affects the rate of output energy. Assuming mirror distance from each other, mirror tilt, position of sun rays, and receiver height, some of the optical losses are detected in the system (see Table 2).

Several researchers have studied the linear Fresnel solar concentrators in both initial and secondary generations (11, 12). A comprehensive review in designing and application of the LFRs has been performed by Bellos et al. (13). In the study on the first generation of Fresnel solar concentrators conducted by Negi et al. (14), two relationships were suggested for the tilt and distance of mirrors in a Fresnel field. The tilt and

distance of mirrors in a Fresnel field could be estimated by simultaneously resolving the mentioned relationships for conditions that the sun rays are normal to the collector. The zero shading and blocking losses, and maximizing the received power are the foundations of the mentioned relationships that were proposed for different receivers, including horizontal, vertical, and multi-tube receivers (15, 16). These relationships were applied only when the rays were normal to the moving plate; thus, the plate below the mirrors rotated such that it was always perpendicular to the sun rays. In other words, the models developed by this group were considered a type of solar island where the mirrors were fixed, and the plate below the mirrors was responsible for tracing the sun rays. They proposed some simple relationships to estimate the received energy and heat transfer (14). The second type of Fresnel concentrator is the new generation that has become the focus of new studies. The Solarmondo experimental power plant was built aimed at validating the ray-tracing of the sun's rays and investigating the corresponding functional and mechanical dimensions. Beltagy (17) studied the effect of glass on mono-tube and bi-tube receivers. In their study, a linear Fresnel prototype, developed by CNIM Company, was used in all tests. The optical field was made of 14 rows of mirrors with were constant distance between mirrors. The results showed that the removal of the receiver glass can increase annual optical efficiency by up to 5.6%. El Gharbi et al. (18)conducted a comparative study on the linear Fresnel solar concentrator with the east-west arrangement and linear parabolic concentrator, without considering the effects induced by shading or blocking the sun's rays. Abbas et al. (19) investigated the characteristics of concentrate in circular mirrors and determined the optimal width of mirrors based on the changed concentrate point in the mirror early and late in the day. Abbas and Martínez-Val (20) conducted an analytical study on the Fresdemo power plant in Spain. They investigated the effect of different parameters applying the ray-tracing methods.

In almost all research studies, the sun's rays are converted into transversal and longitudinal components. Zhu (21) proposed a vector analysis to determine the mentioned components. Ghodbane et al. (22) conducted a one-dimensional and transient numerical simulation on a LFR to evaluate the thermal efficiency, optical efficiency, and output temperature for the steam generator. That research was performed on 12 typical days during the year months for El-Oued, Algeria. Based on the results, the maximum thermal efficiency and optical efficiency were obtained as 37% and 53%, respectively. The curvature of mirrors was studied in some research. Lin et al. (23) constructed a prototype of concave mirrors with a bending radius of 3 m and an absorbent height of 1.5 m above the surface of the mirrors. There was a relatively good agreement between the results obtained by this group and the results reported by Morin et al. (24) where the bending radius was twice the distance between the mirror and the absorber. Heimsath et al. (25) investigated the effects induced by the degree of curvature, receiver height, and distance between mirrors using the ray-tracing methods. In their study, the north-south and east-west arrangements were also investigated. The north-south arrangement was finally considered a promising candidate. Santos et al. (26) performed the optical analysis of a LFR with a flat receiver considering the new analyses of shading, blocking, and cosine losses. The authors developed their analytical analysis in Phyton and compared the results with ray tracing simulations performed in SolTrace for both factorized and biaxial models of intercept factor. The results showed that the larger errors were obtained for high incidence angles ($\theta L \geq 80^{\circ}$). Sharma et al. (27) studied the compact linear Fresnel reflectors (LFRs) with two receivers on both sides of the optical field. They studied different optical field parameters such as the receiver's height, rows of reflectors, length and width of reflectors, and the effect of these parameters on electricity cost. Furthermore, Montes et al. (28) defined some new variables and criteria for analyzing a developed prototype. In their study, the threshold for radiation was 10 kw/h and this was the lowest value to be considered for heating fluid in the absorber. This study was performed for 3 optical fields with different widths and filling factors. Also, a comparison was done between Fresnel concentrators with single receiver and multi-receiver (compact linear Fresnel). It was claimed that although compact Fresnel concentrators have lower shading and blocking losses, these merits cannot outweigh the negative outcomes of the greater dispersion of sun rays (28). Roostaee and Ameri (29, 30) used an analytical method to investigate the dynamic relation between the reflector field and receiver optimum dimension for a constant width and shift arrangement in LFRs with a trapezoidal cavity receiver. They investigated the annual energy and exergy efficiency of Fresnel collectors. Kuchkarov et al. (31) developed a solar power plant module for individual consumers to obtain thermal, mechanical and electrical energy. An approach to determine the dimensions optimal diof flat mirrors was proposed based on the size of the receiver (27-32). Santos et al. (33) proposed a method to increase the amount of concentrated energy by increasing the number of primary concentrators (mirrors). In their research, the characteristics of the mirrors were the same in all the simulations, but with increasing the number of mirrors (total mirror area), the filling factor increased, which resulted in more energy concentration. Kincaida et al. (34) performed a sensitivity analysis on the insensitive parameters of the optical efficiency of a LFR to present insightful guidance for the manufacturing and implementation the optical losses. In that research, the

TABLE 2. Optical losses in the Fresnel concentrators

Loss type	Considerations
Shading	Adjacent mirrors cast shadows on each other[35].
Blocking	Reflection rays collide on the back of front mirrors in their path[30].
Irregular reflection of mirrors	Mirror surfaces do not have a perfectly regular reflection.
Error of solar tracking system	Mechanical system errors and limited accuracy of the device are the reason[24].
Receiver shadow	The receiver's shadow falls on each row of mirrors in a short time[35].

effect of twisting and Tracking errors of primary reflectors, the horizontal displacement of the receiver tube, and the vertical displacement of the secondary reflector on the LFR optical efficacy were investigated. A high-fidelity opto-mechanical error model was presented to obtain the realistic performance of the LFR. Said et al. (35) studied the numerical and experimental analysis of a small LFC considering the important parameters such as the longitudinal and transversal coefficients of the incidence angle modifier, the optical efficiency, and the concentration ratio. They concluded that the optical efficiency of the LFC significantly changes by the number of mirrors; 42.65% for 11 mirrors, 35.82%, and 26.98% for 9 and 7 mirrors, respectively. The previous studies on linear Fresnel concentrators have at least one of the following limitations:

- The existing Fresnel power plants have always been examined from a specific point of view and the effects of other parameters were eliminated (18).
- They tried to reduce the optical losses by defining some specific parameters.
- Optical field materials such as reflecting surface area and field factor were not constant (26, 30).

However, in the present study, the main contributions are as follows:

- Three arrangements with fixed, variable, and optimal spacing between mirrors were examined and compared for Kerman, Iran.
- The characteristics of mirrors, total mirror area, and filling factor were constantan for all arrangements, and it has been tried to achieve higher optical efficiency just by changing the place of mirrors. Also, the width of the field was the same for all three layouts, so that the center of the last mirror was a maximum of 8 meters from the center of the field, the absorber height was 8 m for all arrangements and the width of each mirror was 60 cm.
- It has been tried to achieve the highest optical efficiency by using the genetic algorithm in optimal distance arrangements. Moreover, by merging equations of the first generation of LFRs with the new generation, the variable distance arrangement obtained with the optical efficiency is close to the optimal arrangement.
- A small-scale prototype Fresnel concentrator was developed for practical testing of these three arrangements and comparing them. In the developed model, the location of the mirrors could be changed so that all the layouts could be implemented and checked. After several experiments on each arrangement, the efficiency versus loss parameter curve was finally plotted to compare the performance of these three arrangements in different environmental conditions.

2. NUMERICAL MODELS

In the initial studies on the Fresnel concentrators, all the mirrors were fixed on one plate whose function was to track the sun rays. Such a design requires a huge disc to hold all the mirrors along with a powerful guiding engine, also the disc movement led to receiver movement, highlighting the need to apply deformable connections on both sides of the receiver. The deformable connections led to the loss of the sealing costs and the chance of increasing the pressure up to high values. Changing the tilt of the mirrors in the next generation of Fresnel concentrators results in the concentration of sunlight on the receiver surface. In this design, the optical losses of Fresnel concentrators will be a concern. Section 2 deals with the governing equations related to these generations of Fresnel concentrators.

2. 1. The variable distance design The mirror arrangement in the traditional design of the optical field was in a way that none of the mirrors had shading and blocking losses whenever the disc was normal to the sun rays. Although these concentrators are obsolete due to their disadvantages such as construction costs, huge sun tracker devices, and so on, their optical performance was extremely high, and this was a merit. Therefore, in this study, in the variable distance arrangement, the distance between the mirrors has been calculated from first-generation equations because in conditions where the sun rays are almost perpendicular to the surface (around solar

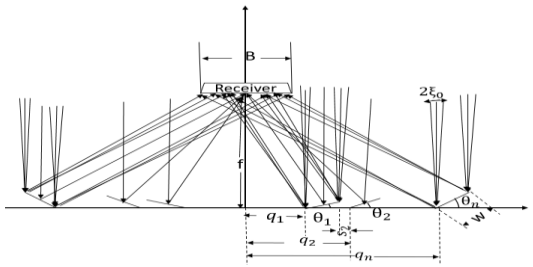

Figure 1. Transverse schematic of a Fresnel field (36)

noon), when the Direct Normal Irradiance (DNI) is also high, zero optical loss plays a vital role in optical performance. But the tilt of the mirrors is calculated according to the new generation relations in such a way that changing the tilted slope of each mirror causes the sun rays to focus on the receiver. In this way, construction difficulties in first-generation are eliminated. Furthermore, by tracking the sun rays during the day, concentrated energy is obtained. The relationships below are obtained for the first mirror using the geometry represented in Figure 1 (36).

$$q_1 = \frac{B}{2} + f \tan(\widehat{\xi_0}) \quad (1)$$

$$\hat{\theta}_1 = \frac{1}{2}\left[tan^{-1}\left(\frac{q_1+\frac{w}{2}\cos(\widehat{\theta_1})}{f-\frac{w}{2}(sin\widehat{\theta_1})}\right)\right] \quad (2)$$

where q_1 is the distance between the first mirror and center, θ_1 is the slope of the first mirror, ξ_0 is the angle of inclination of the sun rays, f is the receiver height, and B and w are the width of the receiver and mirrors, respectively. The first mirror distance from the field center is set as half the width of the receiver. The tilt is also set such that the rays radiated on the mirrors' center reach the receiver center. From the second mirror outwards, the relationships between location and rotation of mirrors are interrelated, and implicit equations should be solved simultaneously (36):

$$s_n = w\ sin(\widehat{\theta_{n-1}})tan\ (2\widehat{\theta_n} + \widehat{\xi_0}) \quad (3)$$

$$q_n = q_{n-1} + w\ cos(\widehat{\theta_{n-1}}) + s_n \quad (4)$$

$$\hat{\theta}_n = \frac{1}{2}\left[tan^{-1}\left(\frac{q_n+\frac{w}{2}cos(\widehat{\theta_n})}{f-\frac{w}{2}sin(\widehat{\theta_n})}\right)\right] \quad (5)$$

where, s_n is the distance between two consecutive mirrors. In this method, only the number of mirrors (n), width of every single mirror, and receiver height are required to design the field.

2. 2. The Constant Distance Design The Fresnel concentrator mirrors are defined based on their location and the mirror's tilt angle at any given time. In this arrangement, the distance between mirrors is equal. According to Figure 2, the slope of mirrors changes to reflect rays radiated on the mirror center to the receiver center. The subsequent mirrors are placed in the position of $X_i + 1$ in priority so that the distance between each of them is defined as P_i. According to the mentioned law of reflection, the line perpendicular to each mirror at its point of rotation coincides with a bisector between radiated rays and the line connecting the mirror center with the receiver center on a transverse plane. Assuming that the vector perpendicular to the mirror creates a $\hat{\beta}$ angle above the horizon, the equations below are obtained as follows (20):

$$\widehat{\beta_i} = \frac{\widehat{\gamma_R}+\hat{S}}{2} \quad (6)$$

$$\widehat{M_i} = \frac{\pi}{2} - \widehat{\beta_i} \quad (7)$$

where, $\widehat{M_i}$ is the slope of the mirror above the horizon at any given time. The mirrors are placed at an identical distance from each other concerning the filling factor of the field.

2. 3. Optimal field arrangement using genetic algorithm A computer program was developed in MATLAB software for the optimization of the LF reflector using the Genetic Algorithm (GA) based on the pertinent input parameters. A genetic algorithm optimization problem is defined bellow (37):

- Minimizing or maximizing the objective function (or functions) included in the vector:

$$F(x) = f_1(x), f_2(x), \dots, f_k(x)$$

- Satisfying the n restrictions of inequality and the m restrictions of equality:

$$\begin{cases} g_i(x) \geq 0 & i = 1, 2, \dots, n \\ h_i(x) = 0 & i = 1, 2, \dots, m \end{cases}$$

where, x is a vector which its elements are the decision variables of the problem.

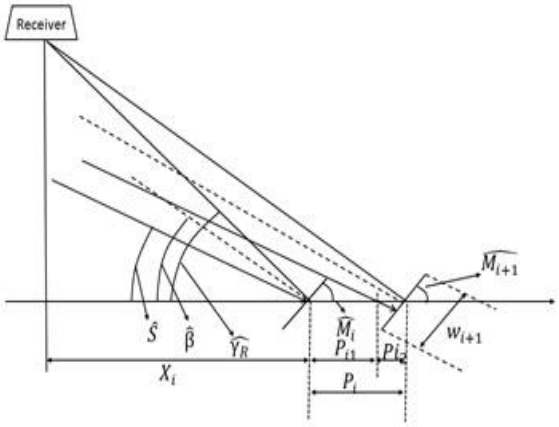

Figure 2. Radiation algorithm in a linear Fresnel concentrator (23)

- **Constrain bounds:**

$$0.55\ cm \le P_i \le 8\ cm$$

where, P_i is the distance between each two mirrors.

The optimization procedure of the GA is presented as follows:

1. Firstly, an initial population is randomly created.
2. Afterwards, a sequence of new populations is created by the algorithm by using the current generation individuals in the next population. The creation of the new population including the scoring of each population member by calculating its fitness value, scaling the raw fitness scores and converting them to the usable ranges, selecting the parents according to the fitness of each member, eliminating the less fitness members (elite), producing the children from the parents (using the mutation or cross over), and replacing the current population with the children to create the next generation.
3. Finally, the algorithm is terminated by applying the stopping criteria.

In this method, an arrangement is selected concerning the practical and spatial limitations, which results in the highest possible concentrated energy under the mentioned conditions. The objective function was annual concentrated energy $\left(F(x) = \sum_{j=1}^{j=8760} Q_{th}\right)$ and the goal was to maximize this objective function or minimize the reciprocal of this. The locations of the mirrors were considered as decision variables (f(x),), which included twelve mirrors on the right side of the field and twelve mirrors on the left side of the field symmetrically. The problem had geometric constraints including the dimensions of the field, so that the total width of the reflector is 255 cm and the distance between each two mirrors could change from 0.55 cm to 8 cm. Also, the location of the mirrors should not interfere with the process of tracking the sun. The genetic algorithm is depicted in Figure 3. In the first stage, some data such as solar data, power plant dimensions and receiver dimensions, and height are read. In the next step, the parameters of the genetic algorithm are determined. These parameters include mutation and crossover, number of iterations, and number and width of mirrors. The first population is then randomly constructed, and then optical losses such as shading of the mirrors and receiver, beam blocking, concentrated energy, and the objective function are calculated. Also, at this stage, the geometric conditions governing the problem are applied and then the answers that do not satisfy the geometric conditions of the problem are removed by applying the λ factor. This cycle is repeated and finally, the decision variables that provide the best objective function are introduced.

2. 4. Adjacent Mirrors Shading The shade created on the mirror depends on the mirror's location, its distance from the adjacent mirror, and its slope. In all examined cases, the axis of rotation of mirrors coincides with their centers at a horizontal surface. As shown in Figure 4 (23), the mirrors with a width of w and the slope of M are positioned in a way that they can reflect the light radiated on the mirror center, on the receiver center at any given time. The value of shadow created at a given time is determined concerning the two adjacent mirrors and geometric considerations.

According to Figure 4, $\hat{S}$ is the angle of the sun's rays above the horizon on the transverse plane, $\widehat{\beta_i}$ is the angle between the axis perpendicular to the mirror and horizon direction, and γ_R is the angle of the line connecting the mirror center and receiver center with the horizon. Considering the geometric relationships between them, the following relations will be obtained (20).

$$\widehat{\gamma_R} = tan^{-1}(\frac{f}{X_i}) \quad (8)$$

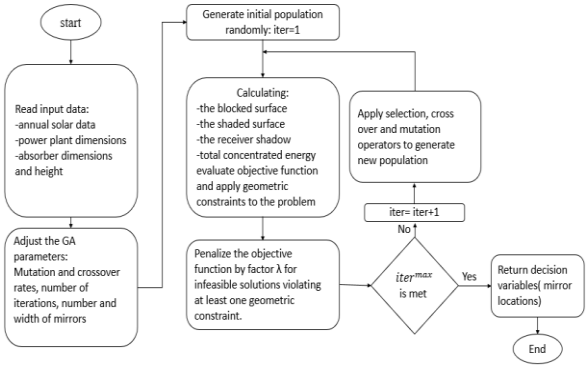

Figure 3. Genetic algorithm flow chart

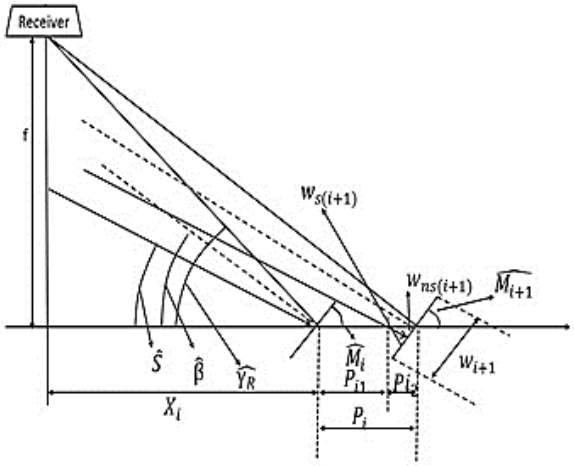

Figure 4. Shading in adjacent mirrors (23)

$$\widehat{\beta_\iota} = \frac{\widehat{\gamma_R} + \hat{S}}{2} \quad (9)$$

$$\widehat{M_\iota} = \frac{\pi}{2} - \widehat{\beta_\iota} \quad (10)$$

where, Equation 10 expresses the tilt of the mirror above the horizon at a given time.

By writing the sine relationships in the triangle specified in Figure 4, the following equation can be expressed (20, 36):

$$p_{i1} = \frac{w_i}{2} . \frac{sin(\pi - \hat{S} - \widehat{M_\iota})}{sin(\hat{S})} \quad (11)$$

The law of sines is used to calculate the value of shadow created on the i+1th mirror. Accordingly, Equation 12 is obtained as follows (20, 36):

$$w_{ns(i+1)} = p_{i2} . \frac{sin(\hat{S})}{sin(\pi - \hat{S} - \widehat{M_{\iota+1}})} \quad (12)$$

where $w_{ns(i+1)}$ is a portion of the $i+1^{th}$ mirror that has no shade.

By substituting $p_{i2} = p_i - p_{i1}$ and Equation 11 into above relation, Equation 13 is expressed as follows (20, 36) [23, 39]:

$$w_{ns(i+1)} = min\left[\left(p_i - \frac{w_i}{2} . \frac{sin\,(\pi - \hat{S} - \widehat{M_\iota})}{sin\,(\hat{S})}\right) . \frac{sin\,(\hat{S})}{sin\,(\pi - \hat{S} - \widehat{M_{\iota+1}})}, \frac{w_{i+1}}{2}\right] \quad (13)$$

The negative value of $w_{ns(i+1)}$ means that the created shadow extends beyond the mirror midpoint. The variable $f_{s(i+1)}$ expresses the ratio of shadowless portion to the surface of the mirror, which is defined based on Equation 14 and varies from zero to one under different conditions (20, 36):

$$f_{s(i+1)} = \frac{\frac{w_{i+1}}{2} - w_{ns(i+1)}}{w_{i+1}} \quad (14)$$

Given the equation defined for shadow, the maximum shadow occurs when $\pi - \hat{S} - \widehat{M_\iota} = \frac{\pi}{2}$, this refers to when the sun, centers of mirrors, and receivers are placed on a single line.

2. 5. Blocking in Adjacent Mirrors Blocking is the incidence of reflected rays on the back of adjacent mirrors on the way to the receiver, which is another factor that is considered in the losses occurred in the Fresnel concentrators. Figure 5 represents the blocking process in the adjacent mirrors. The method taken to define the blocking relation is almost the same as the shading case (20, 36).

$$w_{nb(i+1)} = min\left[\left(p_i - \frac{w_i}{2} . \frac{sin\,(\pi - \widehat{\gamma_{R_{\iota+1}}} - \widehat{M_\iota})}{sin\,(\widehat{\gamma_{R_{\iota+1}}})}\right) . \frac{sin\,(\widehat{\gamma_{R_{\iota+1}}})}{sin\,(\pi - \widehat{\gamma_{R_{\iota+1}}} - \widehat{M_{\iota+1}})}, \frac{w_{i+1}}{2}\right] \quad (15)$$

where, w_{nb} indicates the portion of the mirror that delivers the reflected rays to the receiver. According to Equation 15, the maximum blocking occurs when $\pi - \widehat{\gamma_{R_{\iota+1}}} - \widehat{M_\iota} = \frac{\pi}{2}$, this means when the mirror is perpendicular to the line connecting the centers of the mirror and receiver. The variable $f_{b(i+1)}$ expresses the ratio of blocked surface to the total surface area of the mirror, which is defined based on Equation16 and varies from zero to one under different conditions (20, 36).

$$f_{b(i+1)} = \frac{\frac{w_{i+1}}{2} - w_{nb(i+1)}}{w_{i+1}} \quad (16)$$

2. 6. Overall Loss Coefficient of Adjacent Mirrors The shading and blocking phenomena begin from the bottom of the mirror and then reach the mirror center or even beyond, consequently, when a mirror is simultaneously subjected to shading and blocking phenomena, the one with a more significant coefficient is predominant. These two factors should not be added.

$$f_t = max\,(f_s, f_b) \quad (17)$$

where f_t is the overall loss factor. Then, the optical efficiency of LFR could be obtained as follows (38):

$$\eta_{opt} = \alpha \times \rho_m \times \tau \times (1 - f_t) \quad (18)$$

where, α , ρ_m, and τ are the absorption factor of the receiver tube (0.94), mirror reflectance coefficient (0.92), and Cover glass transmittance (0.95), respectively.

3. EXPERIMENTAL AND SIMULATION SETUPS

3. 1. Measurement Instruments and Uncertainties The measurement tools include the pyranometer, thermometer, flowmeter, and a potentiometer in the tracker system. A CM6B model pyranometer made of Kippzonen was used, which is capable of measuring the irradiation up to 2000 W/m^2 with a measurement uncertainty of 2%. Two thermometers, model PECULA, with stainless steel coils were used to measure the

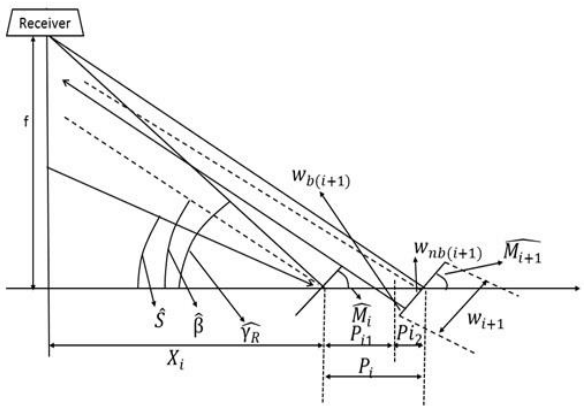

Figure 5. Blocking in adjacent mirrors (20)

temperatures at the inlet and outlet of the LFR absorber. These thermometers could measure the temperature within the range of 50-300\°C with a measurement uncertainty of 0.1\°C. In addition, a 10 kΩ potentiometer was applied in the tacker system which could report the rotational variations with a measurement uncertainty of 0.32 degree. Moreover, all the experiments were conducted under the open-loop conditions. So that the inlet water enters the LFR from the water reservoir with the mass flow rate of 60 L/h. The used flowmeter is model FTB-1424-HT, which measures the volumetric flow rate within the range of 20 L/h to 200 L/h with an uncertainty of 0.7% of the measured value.

3. 2. Design and Construction of a Prototype LFR

The solar collectors' thermal efficiency is determined either theoretically based on the optical and thermal properties of the constituent components or experimentally based on some given conditions. It should be noted that the theoretical thermal evaluation of collectors is accompanied by errors, which occurred at different boundary conditions. However, the theoretical thermal evaluation is always efficient in designing prototypes, and it is necessary to test the designed prototypes concerning different related standards. A small-scale Fresnel concentrator prototype was designed and constructed to compare constant, variable, and optimal distance arrangements. The linear Fresnel concentrator composed of 12 flat mirrors, six mirrors on each side, each with a thickness of 4 mm, width of 17 cm, and length of 180 cm with a total reflection surface area 3.67 m^2 was developed to evaluate the energy obtained in different field arrangements. Also, the total width of the LFR collector is 255 cm. The developed concentrator included three major parts: a concentrating field, a trapezoidal receiver, and a solar tracking system which is depicted in Figure 6. The trapezoidal receiver used in the concentrator had a large base of 28 cm, a small base of 12.8 cm, and a height of 12.5 cm. Three absorption vacuum tubes were used inside the receiver, each with a glass diameter of 58 mm and a steel tube diameter of 42 mm. The vacuum tubes were connected in series such that the working fluid (water) finally exited from the last tube after passing through three return paths. The input and output temperatures were measured using two thermometers with an accuracy of ±0.1 °C.

Mirrors were capable of moving along the frame, so by changing the location of the mirrors, it was possible to implement 3 different layouts. An 8 cm long shaft was located inside a bearing at the end of the frame of every single mirror to rotate the mirrors in order to track the sun's rays at different times. Gears with a module of 2 and 18 teeth with a diameter of 4 cm were embedded at the end of the shaft. The teeth are in contact with a rack above them, which is driven by a linear actuator. The linear actuator is commanded using a control circuit programmed based on the solar data. Feedback seemed necessary due to changes in the speed of the actuator. To do this, a potentiometer of 10 kΩ was used to report the angular changes with an accuracy of 0.3268 degrees. Figure 7 shows the device's solar tracking system.

3. 2. Field Simulation with Ray-tracing Tools

Due to a large number of design parameters and system complexity in solar concentrator systems, it is impossible to physically examine or manufacture numerous practical and economic prototypes. Consequently, using computer codes not only leads to cost savings but also makes it possible to evaluate very complicated systems. Monte Carlo is a statistical method in which the random rays are generated based on the statistical methods. Such rays are generated at different radiation angles, and then the path related to every single ray is traced until it reaches the receiver or is lost in space. In the present study, the SolTrace software was used for simulating the optical field, which uses the Monte Carlo method for tracing the rays [42, 43]. Moreover, the optical properties of the materials used in the simulation of the LFR using SolTrace software are as shown in Table 3.

4. RESULTS

The data reported by Abbas and Martínez[23] on the losses calculated per mirror for Fresdemo power plant were used as reference data for validation of the method

Figure 6. The developed prototype

Figure 7. The developed solar tracking system

used in the present work. Firstly, the Fresdemo power plant in Almeria was considered in validation, in which 12 mirrors were symmetrically arranged on each side of the field with a filling factor of 71.4. According to Figure 8, there is a good agreement between the simulation results and those reported by Abbas and Martinez (20) indicating the accuracy of the applied method.

Then the simulation was done for local data in Kerman, Iran (30°17′N 57°05′E). In the constant distance arrangements (CDA), the distance between the center of the mirrors was considered identical and equal to 67 cm, while based on Equations 4 and 5 in the variable distance arrangement (VDA), the distance of the mirrors was calculated. In the optimal distance arrangements (ODA), the distances between mirrors were obtained using the genetic algorithm. The locations of 12 mirrors, which are the distances between the center of the mirrors and the center of the field on the right side of the field are presented in Table 4 for three arrangements. These distances are repeated exactly for the 12 mirrors on the left side.

The mirrors, which are farther from the center of the field, have more losses due to the sharper tilt angles during the day. Therefore, for the end mirrors, more distance is needed between these mirrors to minimize these losses. In variable and optimal distance arrangements, the distance between the mirrors gradually increases, which reduces optical losses while in constant distance arrangement, all distances between mirrors are equal. Figure 9 represents the shading and blocking in the first, sixth, and twelfth mirrors on the east side of the field in the constant, variable, and optimal distance arrangements concerning the receiver shading.

The Y-axis of Figures 9, 10, and 11 shows the total unblocked or unshaded mirror width which performs the reflection. The value of 0.6 m indicates that all mirrors with a total width of 0.6 m and without optical losses reflect the incident energy. The values lower than 0.6 m

TABLE 1. The optical properties of materials used in SolTrace

Properties	Value
Primary and secondary mirror reflectivity	0.95
Absorber tubes absorbance	0.94
External diameter of absorber tube	0.058 m
Internal diameter of absorber tube	0.042 m
Primary and secondary mirror transmissivity	0
Slope error	0.95 m rad
Specularity error	0.0001
Error type	Gaussian

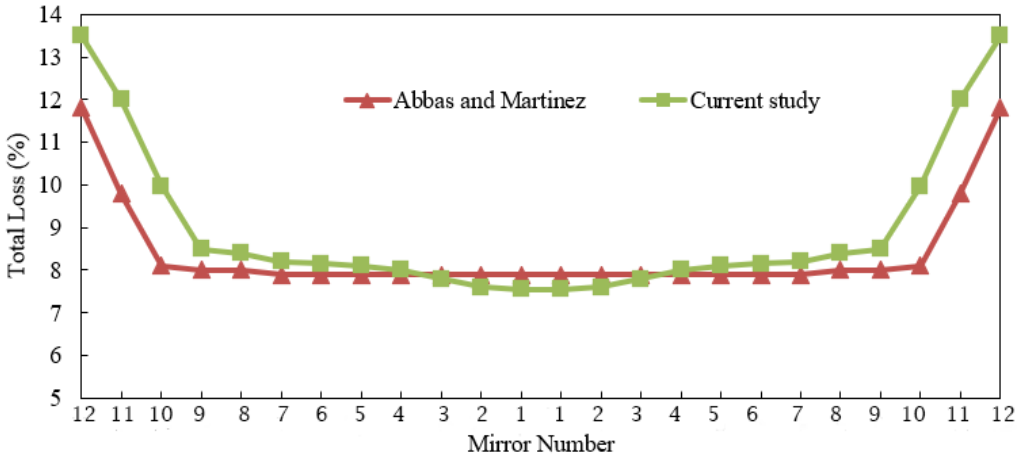

Figure 8. Comparison of percentage of energy losses in the field mirrors in the present study and the one conducted by Abbas and Martínez (20)

TABLE 4. Location of mirrors in the different field arrangements

Mirror number	1th	2th	3th	4th	5th	6th	7th	8th	9th	10th	11th	12th
	Mirrors distances											
CDA (m)	0.60	1.27	1.94	2.61	3.28	3.95	4.62	5.29	5.96	6.63	7.30	7.97
VDA (m)	0.63	1.24	1.84	2.46	3.09	3.73	4.38	5.06	5.76	6.48	7.23	7.98
ODA (m)	0.55	1.22	1.83	2.45	3.09	3.74	4.40	5.10	5.80	6.51	7.25	8.00

in Figures 9,10, and 11 show that only part of the width of the total mirrors participates in the reflection, thereby part of the incident energy is lost. According to the Figures 9,10, and 11 in the constant distance arrangement, just the central mirrors of the field concentrate more energy, while the last mirrors have severe losses of shading and blocking and have a small share in the total concentrated energy. However, mirrors with the optimal and variable distance arrangement generally operated better and produced more energy since the last mirrors produced almost the same energy as central mirrors of the field concentrate more energy, while the last mirrors have severe losses of shading and blocking and have a small share in the total concentrated energy. However, mirrors with the optimal and variable distance arrangement generally operated better and produced more energy since the last mirrors produced almost the same energy as central mirrors. The concentrated energy in the sixth mirror is almost the same for all arrangements because

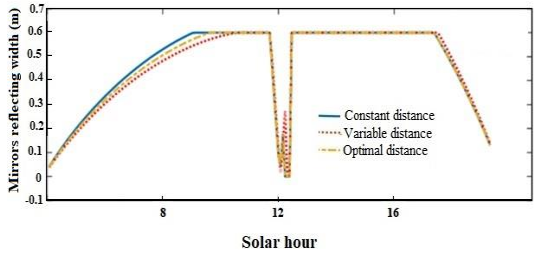

Figure 1. Shading or blocking on June 21 in the first mirror, numerical results

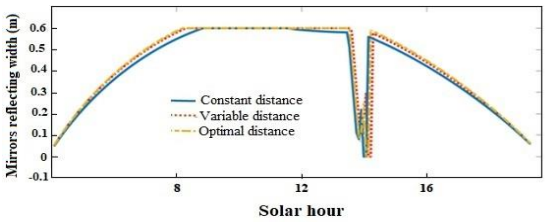

Figure 2. Shading or blocking on June 21 in the sixth mirror, numerical results

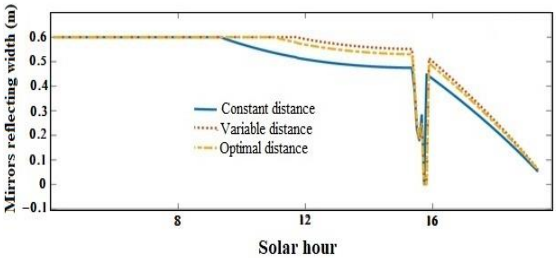

Figure 3. Shading or blocking on June 21 in the twelfth mirror, numerical results

according to the curve gradients, shading has the greatest effect on the central mirrors, while blocking is more common on the end mirrors. Moreover, the performance of the last mirrors in the variable arrangement is very close to the optimal arrangement since the distance between mirrors gradually increases in these two arrangements.

The graph breaks show the effect of the receiver shadow. In some cases, the receiver's shadow overlaps with the losses caused by shading and blocking, and sometimes the receiver's shadow casts shadows on the parts that do not have the shading or blocking losses, in which case the maximum loss results.

By comparing the energy obtained in the various arrangements, it was concluded that the efficiency of concentrated energy in the optimal distance arrangement is about 1.3% and 0.8% higher than the constant distance and variable distance respectively. It should be mentioned that these values were calculated considering the effects induced by blocking and shading of mirrors and the receiver. Figure 10 represents the ratio of energy concentrated by each of the mirrors concerning different arrangements. According to Figure 12, while in the constant distance arrangement central mirrors have greater performance than the variable and optimal distance arrangements, the end mirrors are less involved in the concentrated energy. However, almost all mirrors are equally involved in the final output energy in the variable and optimal distance arrangement. This can be justified by the fact that in the variable and optimal distance arrangement, the effects induced by shading and blocking are reduced in the field edges as the distance between mirrors increases. In the constant distance arrangement, the end mirrors lose much of their reflective surface due to the effects induced by severe shading and blocking. The overall efficiency of the collector and its changes during the year are of special importance. Figure 13 shows the annual changes in the optical efficiency of the collector in three configurations.

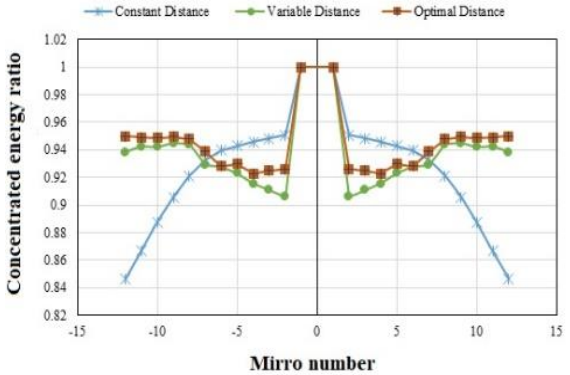

Figure 12. The mirrors energy shares in constant, variable and optimal distance arrangements, numerical results

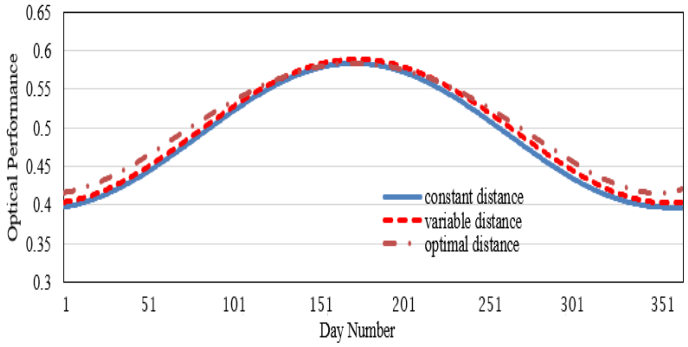

Figure 13. The yearly daily average optical efficiency in constant, variable and optimal distance arrangements, numerical results

According to Figure 13 all three arrangements have higher optical performance in the middle of the year than in the beginning and end of the year due to the angle of the sun and the losses caused by the transmission of the sun's rays to the mirror plates. Moreover, in the first and last days of the year, there is more difference in various layouts, while in the middle of the year, the optical efficiency of different layouts is almost the same. In general, the optical efficiency in the optimal distance arrangements is maximum and the fixed arrangement efficiency between the mirrors has the lowest efficiency, but in the middle of the year, the variable distance arrangement has a better performance than the optimal distance arrangement and different arrangement curves in some places are intertwined.

To assess the effect of beam spread, the constant and variable distance arrangements were separately modeled using the SolTrace software. It should be noted that in both layouts with variable and optimal spacing, the distance between mirrors gradually increases, and both layouts behave similarly in this regard, so only the results of the variable and constant distance arrangements are given. Figures 14 and 15 represent the concentration of energy in the constant and variable distance arrangements. The red rays indicate the reflections that do not reach the receiver. The optical profile of the back surface of mirrors is also defined as the front surface of mirrors to specify the blocked rays, which is why the red rays are reflected downwards. According to the figures, the lost rays occur mostly in the constant distance arrangement, particularly in the end mirrors. However, in the variable distance arrangement, deviations occur because of the mirrors' roughness and large distance of end mirrors.

Figures 16, 17 , 18 and 19 represent the flux distribution in the receiver for constant and variable distance arrangements.

As can be seen, because of using flat mirrors, the created flux is almost uniformly distributed on the receiver in both constant and variable distance arrangements, and there is no difference in the receiver center and its edges. In order to test the desired layouts, a small-scale prototype was designed in such a way that the location of the mirrors could be changed to test different arrangements. Each of the layouts was tested in May

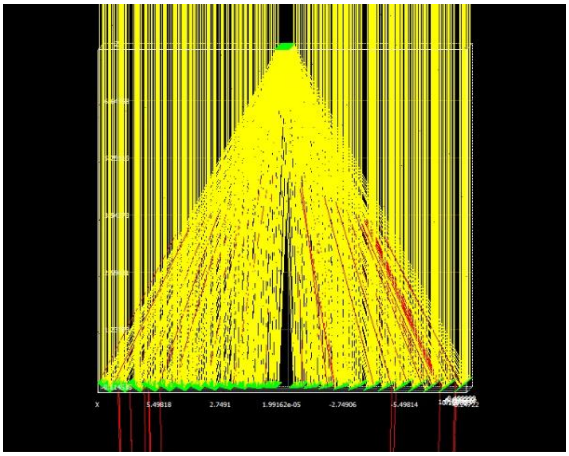

Figure 4. Energy concentration in the constant distance arrangement, simulation results

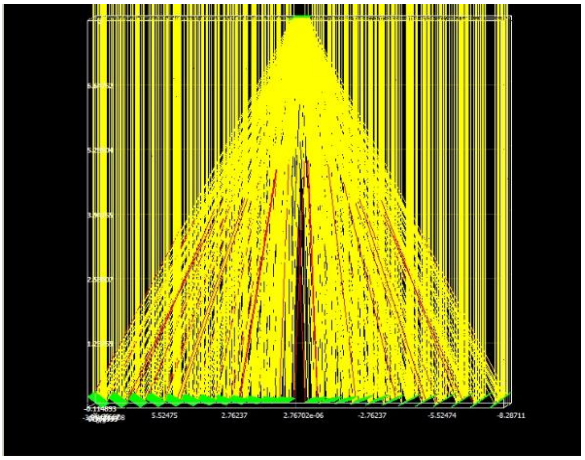

Figure 5. Energy concentration in the variable distance arrangement, simulation results

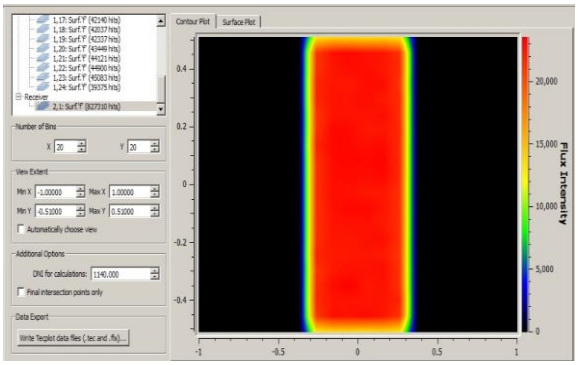

Figure 6. The receiver flux contour in the constant distance arrangement, simulation results

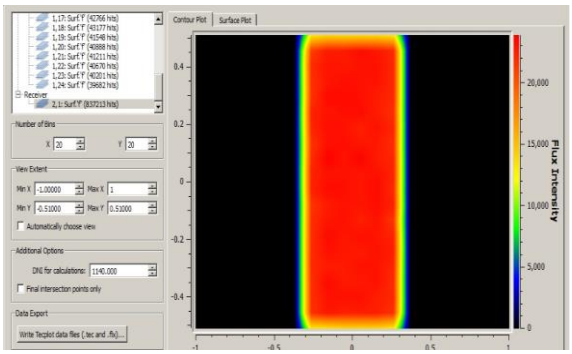

Figure 7. The receiver flux contour in the variable distance arrangement, simulation results

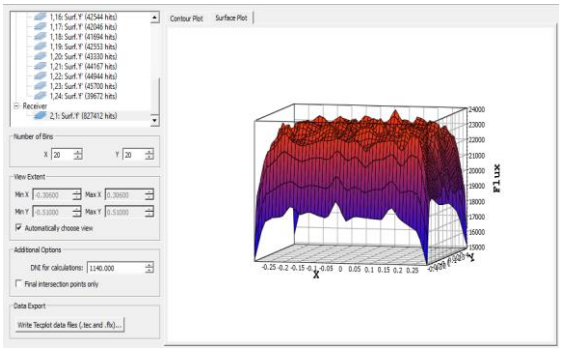

Figure 8. Surface distribution of radiation incident on the receiver in the constant distance arrangement, simulation results

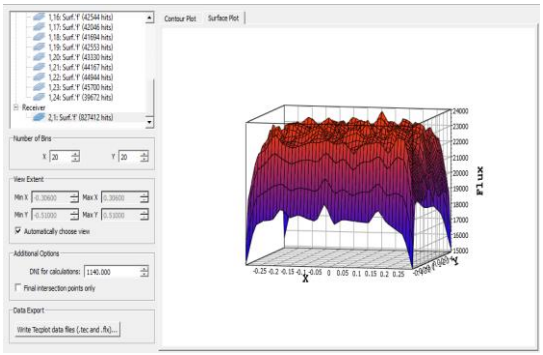

Figure 9. Surface distribution of radiation incident on the receiver in the variable distance arrangement, simulation results

from 10 a.m. to 2 p.m. in Kerman (57.05 °E, 30.17 °N), while the time step was 15 minutes. Experiments were performed with north-south orientation in a closed loop, in which the following parameters were measured in each step: total solar radiation on the collector plate (G_t) diffuse solar radiation on the collector plane (G_d), ambient air temperature (T_a), Operating fluid inlet temperature (T_i), Operating fluid outlet temperature (T_o), and water flow ($\dot{m}$). By dividing the useful energy received by the input energy, the collector efficiency is obtained according to Equation 19.

$$\eta = \frac{\dot{m}c_p(T_o - T_i)}{A_a G_b} \quad (19)$$

In Equation 19 G_b is equal to the difference between G_t and G_d.

Graph η according to the loss parameter $(T_i - T_a)/G_b$ is drawn as a curve whose intersection with the vertical axis occurs when the inlet fluid temperature is equal to the ambient temperature and maximum efficiency occurs in these circumstances. The test results are shown in Figure 20. This figure represents the changes in the concentrator efficiency in terms of loss parameter. The specified points indicate the experimentally obtained points. The results obtained from the experimental tests are denoted by the small squares, triangles, and crosses in Figure 15 corresponding to the variable distance, optimal distance, and constant distance scenarios, respectively. By using a curve-fitting method (second-order polynomial fit), the curve that best fits the points are obtained for the LFR thermal efficiency (4), which are subsequently presented as Equations 20 to 22.

In the constant, variable and optimal distance arrangements, the equations of the second-degree curves are defined through Equations 20, 21 and 22, respectively.

$$\eta = 0.4503 - 0.0025\left(\frac{T_i - T_a}{G_b}\right) - (5.10^{-5})\frac{(T_i - T_a)^2}{Gb} \quad (20)$$

$$\eta = 0.5432 - 0.0028\left(\frac{T_i - T_a}{G_b}\right) - (6.10^{-5})\frac{(T_i - T_a)^2}{Gb} \quad (21)$$

$$\eta = 0.5577 - 0.0055\left(\frac{T_i - T_a}{G_b}\right) - (2.10^{-5})\frac{(T_i - T_a)^2}{Gb} \quad (22)$$

The constant distance arrangement has an efficiency of 45% under the best conditions, which is the least compared to the other two arrangements because, in constant arrangements, the last mirrors have great losses since there is not enough gap between them. Furthermore, central mirrors have unnecessarily large spaces and the sun rays should pass a larger distance to reach the receiver, this leads to larger spread of reflected rays; also, tracking system errors for first mirrors are

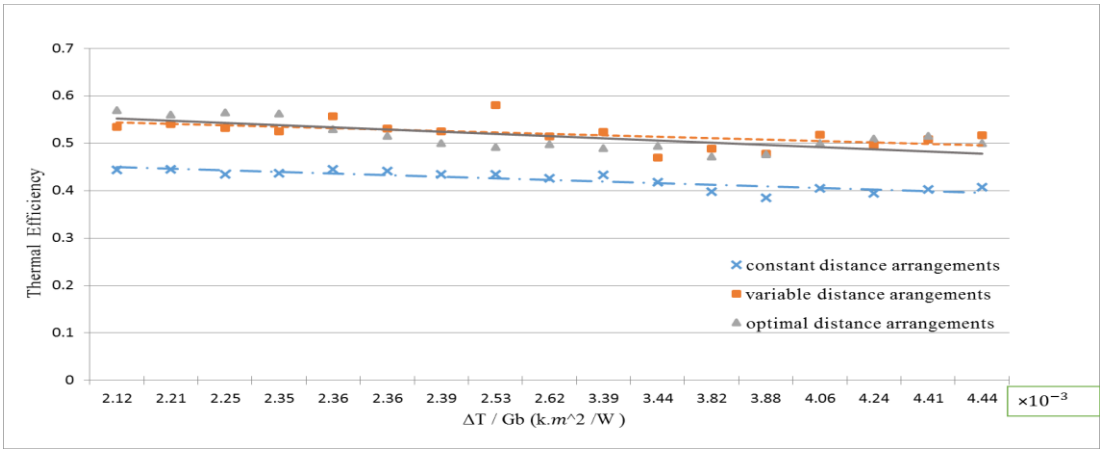

Figure 20. Thermal efficiency in terms of inlet water and ambient temperature difference obtained from the experimental tests

greater due to a larger distance between the mirrors and the receiver. In the results obtained from the experiment and simulation, the arrangement with the optimal distance between the mirrors has the highest efficiency, while the arrangement with the fixed distance between the mirrors has the lowest efficiency and a good agreement was observed between experiment and simulation. Since the width and the number of mirrors are small, the distance between mirrors in the optimal arrangement is mainly close to the variable arrangement so that they have almost the same performance, and their curves are intertwined in many points. Under the best conditions when the temperature of the working fluid is equal to the ambient, the variable and optimal distance arrangements have an efficiency of 54% and 55%, respectively. In these arrangements, the central mirrors are closer to each other, and these gaps are enough for the central mirrors to be out of the shading or blocking of the adjacent mirrors. The remaining space is used in the outer mirrors and they have greater distance in comparison with central mirrors. As a result, the field efficiency increases while the field width remains constant.

3. CONCLUSION

In the present study, three types of field arrangement with constant, variable, and optimal distance between mirrors was examined through a year while field dimensions were equal for the three arrangements. It is shown that:

To track the sun, the outer mirrors in the field always have a sharper angle than the central mirrors, and as a result, more optical losses occur in them.

- In the fixed-distance field layout, in which all mirrors have the same distance from each other, has large losses in the end mirrors, and these mirrors have a lower share of concentrated energy.
- In variable spacing, the distance between the mirrors gradually increases as they move toward the end mirrors, resulting in less loss in this arrangement than in fixed distance arrangement.
- In optimal field spacing, using the genetic algorithm and optimizing the amount of output energy, the location of each mirror was determined, and the simulation results indicated 1.2% and 0.8% efficiency improvement in comparison with constant distance and variable distance, respectively.
- The ray tracing simulation results showed that the end mirrors have a lot of optical loss compared to the central mirrors, and these losses had the highest value in the fixed distance arrangement and the lowest value in the optimal distance.
- The experimental results showed that the field arrangement at constant distance has a maximum efficiency of 45%, variable distance has a maximum efficiency of 54% and optimal layout has a maximum efficiency of 55%, so using genetic algorithms in the arrangement of the optical field of Fresnel concentrators can have a significant impact on the efficiency of these concentrators, although it does not increase costs. Moreover, the use of variable distance arrangements can be used as an efficient method in the design of Fresnel concentrators, which results in much better results than the fixed distance arrangement, and even on small scales has thermal efficiency close to optimal arrangement.

The future direction of the current study is to investigate the influence of using different nanofluids on the overall efficiency of the system.

4. REFERENCES

1. Sadeghi S, Baniasad Askari I. Performance and economic investigation of a combined phosphoric acid fuel cell/organic Rankine cycle/electrolyzer system for sulfuric acid production; Energy-based organic fluid selection. International Journal of Energy Research. 2020;44(4):2704-25. https://doi.org/10.1002/er.5073

2. Khaligh Fard S, Ahmadi H, Alizadeh Elizei MH. Electricity Supply Model of Conventional Residential Buildings in Tehran with Priority on Renewable Energy Using Adaptive Fuzzy-neural Inference System. International Journal of Engineering, Transactions A: Basics. 2023;36(10):1793-814. 10.5829/ije.2023.36.10a.07
3. Assari M, Mirzavand R, Basirat Tabrizi H, Jafar Gholi Beik A. Effect of steps height and glass cover angle on heat transfer performance for solar distillation: Numerical study. International Journal of Engineering, Transactions A: Basics. 2022;35(1):237-47. https://doi.org/10.5829/ije.2022.35.01A.23
4. Kalogirou SA. Solar energy engineering: processes and systems: Academic press; 2013.
5. Zhang H, Baeyens J, Degrève J, Cacères G. Concentrated solar power plants: Review and design methodology. Renewable and sustainable energy reviews. 2013;22:466-81. https://doi.org/10.1016/j.rser.2013.01.032
6. Sadeghi S, Askari IB. Parametric thermodynamic analysis and economic assessment of a novel solar heliostat-molten carbonate fuel cell system for electricity and fresh water production. Environmental Science and Pollution Research. 2022;29(4):5469-95. https://doi.org/10.1007/s11356-021-16035-2
7. Askari IB, Calise F, Vicidomini M. Design and comparative techno-economic analysis of two solar polygeneration systems applied for electricity, cooling and fresh water production. Energies. 2019;12(22):4401. https://doi.org/10.3390/en12224401
8. Negi B, Kandpal T, Mathur S. Designs and performance characteristics of a linear Fresnel reflector solar concentrator with a flat vertical absorber. Solar & wind technology. 1990;7(4):379-92. https://doi.org/10.1016/0741-983X(90)90023-U
9. Bellos E, Tzivanidis C, Moghimi M. Reducing the optical end losses of a linear Fresnel reflector using novel techniques. Solar Energy. 2019;186:247-56. https://doi.org/10.1016/j.solener.2019.05.020
10. Ma J, Chang Z, editors. Understanding the effects of end-loss on linear Fresnelcollectors. IOP Conference Series: Earth and Environmental Science; 2018: IOP Publishing. 10.1088/1755-1315/121/5/052052
11. Mokhtar G, Boussad B, Noureddine S. A linear Fresnel reflector as a solar system for heating water: theoretical and experimental study. Case Studies in Thermal Engineering. 2016;8:176-86. https://doi.org/10.1016/j.csite.2016.06.006
12. Said Z, Ghodbane M, Tiwari AK, Ali HM, Boumeddane B, Ali ZM. 4E (Energy, Exergy, Economic, and Environment) examination of a small LFR solar water heater: An experimental and numerical study. Case Studies in Thermal Engineering. 2021;27:101277. https://doi.org/10.1016/j.csite.2021.101277
13. Bellos E. Progress in the design and the applications of linear Fresnel reflectors–A critical review. Thermal Science and Engineering Progress. 2019;10:112-37. https://doi.org/10.1016/j.tsep.2019.01.014
14. Negi B, Mathur S, Kandpal T. Optical and thermal performance evaluation of a linear Fresnel reflector solar concentrator. Solar & wind technology. 1989;6(5):589-93. https://doi.org/10.1016/0741-983X(89)90095-7
15. Mathur S, Kandpal T, Negi B. Optical design and concentration characteristics of linear Fresnel reflector solar concentrators—I. Mirror elements of varying width. Energy Conversion and Management. 1991;31(3):205-19. https://doi.org/10.1016/0196-8904(91)90075-T
16. Mathur S, Kandpal T, Negi B. Optical design and concentration characteristics of linear Fresnel reflector solar concentrators—II. Mirror elements of equal width. Energy Conversion and Management. 1991;31(3):221-32. https://doi.org/10.1016/0196-8904(91)90076-U
17. Beltagy H. The effect of glass on the receiver and the use of two absorber tubes on optical performance of linear fresnel solar concentrators. Energy. 2021;224:120111. https://doi.org/10.1016/j.energy.2021.120111
18. El Gharbi N, Derbal H, Bouaichaoui S, Said N. A comparative study between parabolic trough collector and linear Fresnel reflector technologies. Energy Procedia. 2011;6:565-72. https://doi.org/10.1016/j.egypro.2011.05.065
19. Abbas R, Montes M, Piera M, Martínez-Val J. Solar radiation concentration features in Linear Fresnel Reflector arrays. Energy Conversion and Management. 2012;54(1):133-44. https://doi.org/10.1016/j.enconman.2011.10.010
20. Abbas R, Martínez-Val J. Analytic optical design of linear Fresnel collectors with variable widths and shifts of mirrors. Renewable Energy. 2015;75:81-92. https://doi.org/10.1016/j.renene.2014.09.029
21. Zhu G. Development of an analytical optical method for linear Fresnel collectors. Solar Energy. 2013;94:240-52. https://doi.org/10.1016/j.solener.2013.05.003
22. Ghodbane M, Boumeddane B, Said Z, Bellos E. A numerical simulation of a linear Fresnel solar reflector directed to produce steam for the power plant. Journal of cleaner production. 2019;231:494-508. https://doi.org/10.1016/j.jclepro.2019.05.201
23. Lin M, Sumathy K, Dai Y, Wang R, Chen Y. Experimental and theoretical analysis on a linear Fresnel reflector solar collector prototype with V-shaped cavity receiver. Applied Thermal Engineering. 2013;51(1-2):963-72. https://doi.org/10.1016/j.applthermaleng.2012.10.050.
24. Morin G, Dersch J, Platzer W, Eck M, Häberle A. Comparison of linear Fresnel and parabolic trough collector power plants. Solar energy. 2012;86(1):1-12. https://doi.org/10.1016/j.solener.2011.06.020
25. Heimsath A, Bern G, Van Rooyen D, Nitz P. Quantifying optical loss factors of small linear concentrating collectors for process heat application. Energy Procedia. 2014;48:77-86. https://doi.org/10.1016/j.egypro.2014.02.010
26. Santos AV, Canavarro D, Horta P, Collares-Pereira M. An analytical method for the optical analysis of Linear Fresnel Reflectors with a flat receiver. Solar Energy. 2021;227:203-16. https://doi.org/10.1016/j.solener.2021.08.085
27. Sharma V, Khanna S, Nayak JK, Kedare SB. Effects of shading and blocking in compact linear fresnel reflector field. Energy. 2016;94:633-53. https://doi.org/10.1016/j.energy.2015.10.098
28. Montes MJ, Rubbia C, Abbas R, Martínez-Val JM. A comparative analysis of configurations of linear Fresnel collectors for concentrating solar power. Energy. 2014;73:192-203. https://doi.org/10.1016/j.energy.2014.06.010
29. Roostaee A, Ameri M. Effect of Linear Fresnel Concentrators field key parameters on reflectors configuration, Trapezoidal Cavity Receiver dimension, and heat loss. Renewable Energy. 2019;134:1447-64. https://doi.org/10.1016/j.renene.2018.09.053
30. Roostaee A, Ameri M. A comparative study of different optimised mirrors layouts of Linear Fresnel concentrators on annual energy and exergy efficiencies. International Journal of Ambient Energy. 2022;43(1):2627-44.
31. Kuchkarov A, Abdumuminov A, Abdurakhmanov A. Developing a Design of a Composite Linear Fresnel Mirror Concentrating System. Applied Solar Energy. 2020;56:192-7. 10.3103/S0003701X20030056
32. Sharma V, Nayak JK, Kedare SB. Effects of shading and blocking in linear Fresnel reflector field. Solar Energy. 2015;113:114-38.
33. Santos AV, Canavarro D, Collares-Pereira M. The gap angle as a design criterion to determine the position of linear Fresnel

primary mirrors. Renewable Energy. 2021;163:1397-407. https://doi.org/10.1016/j.renene.2020.09.017

34. Kincaid N, Mungas G, Kramer N, Zhu G. Sensitivity analysis on optical performance of a novel linear Fresnel concentrating solar power collector. Solar Energy. 2019;180:383-90. https://doi.org/10.1016/j.solener.2019.01.054
35. Said Z, Ghodbane M, Hachicha AA, Boumeddane B. Optical performance assessment of a small experimental prototype of linear Fresnel reflector. Case Studies in Thermal Engineering. 2019;16:100541. https://doi.org/10.1016/j.csite.2019.100541
36. Mathur S, Negi B, Kandpal T. Geometrical designs and performance analysis of a linear Fresnel reflector solar concentrator with a flat horizontal absorber. International journal of energy research. 1990;14(1):107-24. https://doi.org/10.1002/er.4440140111
37. Goel A, Manik G. Step towards sustainability: Techno-economic optimization of a parabolic trough solar collector using multi-objective genetic algorithm. Thermal Science and Engineering Progress. 2023;37:101539. https://doi.org/10.1016/j.tsep.2022.101539
38. Rungasamy A, Craig K, Meyer JP. A review of linear Fresnel primary optical design methodologies. Solar Energy. 2021;224:833-54. https://doi.org/10.1016/j.solener.2021.06.021

Persian Abstract

چکیده

در بازتابنده های فرنل خطی، آرایش میدان تاثیر بسزایی بر بازده نوری دارد. سه طرح فاصله ثابت، بهینه و متغیر برای نیروگاه خورشیدی Fresdemo پیشنهاد شده است. مطالعه به صورت شبیه سازی و آزمایش انجام شده است. متمرکز کننده فرنل در مقیاس کوچک با قابلیت اجرای این سه ترتیب طراحی و ساخته شد. راندمان نوری نیروگاه خورشیدی با فاصله بهینه، متغیر و ثابت بین آینه ها با در نظر گرفتن شرایط ثابت برای همه چیدمان ها از جمله ابعاد کلی نیروگاه، عرض و تعداد آینه ها و ابعاد گیرنده مقایسه شده است. مشاهده شد که چیدمان با فاصله بهینه، متغیر و ثابت دارای بیشترین تا کمترین بازده انرژی است. علاوه بر این، آینه های دورتر از مرکز به دلیل زوایای شیب تیزتر تلفات بیشتری را به همراه دارند، بنابراین برای کاهش تلفات به فضاهای بیشتری بین این آینه ها نیاز است. این در حالی است که آخرین آینه ها در آرایش فاصله ثابت دارای تلفات شدید سایه و بلوکه شدن هستند در حالی که در آرایش فاصله بهینه و متغیر تقریباً انرژی معادل با آینه های مرکزی تولید می کنند. نتایج تجربی نمونه اولیه توسعه‌یافته نشان داد که راندمان حرارتی برای فاصله بهینه بالاترین بود، در حالی که چیدمان با فاصله متغیر بازدهی تقریبا مشابه داشت و چیدمان فاصله ثابت کمترین بازده حرارتی را داشت. علاوه بر این، چیدمان فاصله متغیر و بهینه به ترتیب بازدهی ٥٤٪ و ٥٥٪ را نشان دادند.